

Machine Learning Based Blind Decoding for Space–Time Line Code (STLC) Systems

Jingon Joung ¹, Senior Member, IEEE,
and Bang Chul Jung ², Senior Member, IEEE

Abstract—In this correspondence paper, a novel machine learning (clustering) based blind decoding method is proposed for the space–time line code (STLC) systems without the information of modulation size and channels. The number of clusters, which is equivalent to the modulation size, is estimated from the received signals by using a k -mean cluster validation metrics, such as silhouette score and Davies–Bouldin index, and the cluster indices are directly mapped to the transmitted binary information bits. To improve the clustering performance, received signal normalization and the initial centroids of the clusters are designed by exploiting the combined STLC signal structure. From the numerical results, it is verified that the proposed blind decoding method can achieve near-coherent decoding performance with either small-size modulation, low noise at the receiver, or a large number of transmit antennas.

Index Terms—Machine learning, clustering, k -mean algorithm, blind decoding, space–time line code.

I. INTRODUCTION

Recently, various machine learning techniques have been applied to the communication systems. For examples, a support vector machine (SVM) is applied for antenna selection [1], reinforcement learning for evolved NodeB selection [2], and deep learning for the multiple access, channel estimation and allocation, and traffic control [3]–[6].

In this study, by employing a machine learning technique, we propose a blind decoding method for the full-spatial-diversity achieving space–time line code (STLC) systems [7]–[11]. The proposed blind decoding method does not require the channel state information (CSI) and modulation information, namely the modulation type and size. The conventional STLC receiver decodes the transmitted information bits with the partial CSI, i.e., an effective channel gain, and the modulation information. Unlike an automatic modulation classification method (see [12] and references therein) that uses a supervised learning algorithm with training, we consider an unsupervised learning method, i.e., k -mean clustering [13], by exploiting the structure of the combined STLC signals.

The number of clusters, which can be interpreted as the modulation size, is determined based on a Davies–Bouldin (DB) validity index and silhouette score [14], [15]. To improve the performance and fast-and-accurate convergence of the clustering, we apply a signal normalization technique and design the initial cluster centroids. Then, the

cluster indices of the normalized signals are mapped to the transmitted information bits, i.e., a decoding step. Numerical results verify that the proposed blind decoding method can achieve the bit-error-rate (BER) performance of a coherent decoding system that uses the information of modulation and channels, especially when the modulation size or the noise at the receiver is small or the number of transmit antennas is large.

II. SIGNAL MODELS OF STLC SYSTEMS

We consider an STLC system, in which a transmitter has N transmit antennas, while a receiver has two receive antennas. The transmitter modulates the coded/uncoded information bits to symbols, denoted by x , and generates the STLC symbols, denoted by s . One resource block (RB) consists of K symbols, and T RBs constitutes one frame. The STLC system transmitter transmits frame by frame discontinuously. The channel is assumed to be static over one RB, yet it varies over different RBs, i.e., quasi-static or block fading channels.

A. STLC Transmission and Received Signal Model

Let $h_{r,n}[t]$ be the channel gain of RB t between the n th transmit antenna and the r th receive antenna, where $n \in \{1, \dots, N\}$, $r \in \{1, 2\}$ and $t \in \{1, \dots, T\}$. The channel $h_{r,n}[t]$ is an independent and identically distributed (i.i.d.) complex Gaussian random variable with zero mean and unit variance, i.e., $h_{r,n}[t] \sim \mathcal{CN}(0, 1)$. Consider an M -size modulation, i.e., M alternative symbols exist on a constellation diagram. $\log_2 M$ information bits are modulated to one of M symbols, x , which conforms to $E[x] = 0$ and $E[|x|^2] = 1$.

We consider the STLC processing of x for the t th RB of the n th transmit antenna. Note that the channels are static within one RB and the STLC processing of all antennas are identical to one another. The K consecutive STLC symbols transmitted through antenna n are obtained by the STLC processing with CSI $\mathbf{h}_n[t] = [h_{1,n}[t] h_{2,n}[t]]^T$ as follows [7]–[11] ($k' = 1 \dots, K/2$):

$$\begin{bmatrix} s_{2k'-1,n}^*[t] \\ s_{2k',n}[t] \end{bmatrix} = \frac{1}{\|\mathbf{h}_n[t]\|} \begin{bmatrix} h_{1,n}[t] & h_{2,n}[t] \\ h_{2,n}^*[t] & -h_{1,n}^*[t] \end{bmatrix} \begin{bmatrix} x_{2k'-1}^*[t] \\ x_{2k'}[t] \end{bmatrix}, \quad (1)$$

where $s_{k,n}[t]$ is the STLC symbol transmitted through the n th transmit antenna at the k th symbol transmission time of RB t , such that $E|s_{k,n}[t]|^2 = 1, \forall n$.

The received signal of the k th symbol in RB t at receive antenna r is then written as follows ($r = \{1, 2\}$, $k = \{1, \dots, K\}$, and $t = \{1, \dots, T\}$):

$$y_{r,k}[t] = \sum_{n=1}^N h_{r,n}[t] s_{k,n}[t] + v_{r,k}[t], \quad (2)$$

where $v_{r,k}[t]$ represents an i.i.d. complex additive white Gaussian noise (AWGN) that conforms to a normal distribution with a zero mean and variance σ_v^2 , i.e., $v_{r,k}[t] \sim \mathcal{CN}(0, \sigma_v^2)$.

B. Combined STLC Signal Model

Using (1) to (2), we can specifically represent the received signals at receive antenna r for the even ($k = 2k'$) and odd ($k = 2k' - 1$) time

Manuscript received January 1, 2019; accepted March 13, 2019. Date of publication March 18, 2019; date of current version May 28, 2019. This work was supported in part by the National Research Foundation of Korea (NRF) funded by the Korea government (MSIT) under Grant NRF-2016R1D1A1B03930250 and in part by the Basic Science Research Program through the NRF funded by the Ministry of Science and ICT under Grant NRF-2016R1A2B4014834. The review of this paper was coordinated by Prof. G. Gui. (Corresponding author: Bang Chul Jung.)

J. Joung is with the School of Electrical and Electronics Engineering, Chung-Ang University, Seoul 06974, South Korea (e-mail: jgjoung@cau.ac.kr).

B. C. Jung is with the Department of Electronics Engineering, Chungnam National University, Daejeon 34134, South Korea (e-mail: bcjung2@cnu.ac.kr).

Digital Object Identifier 10.1109/TVT.2019.2905622

signals as follows ($k' = 1, \dots, K/2$):

$$y_{r,2k'-1}[t] = \sum_{n=1}^N \frac{h_{r,n}[t]}{\|\mathbf{h}_n[t]\|} (h_{1,n}^*[t]x_{2k'-1}[t] + h_{2,n}^*[t]x_{2k'}^*[t]) + v_{1,2k'-1}[t], \quad (3a)$$

$$y_{r,2k'}[t] = \sum_{n=1}^N \frac{h_{r,n}[t]}{\|\mathbf{h}_n[t]\|} (h_{2,n}^*[t]x_{2k'-1}^*[t] - h_{1,n}^*[t]x_{2k'}[t]) + v_{1,2k'}[t]. \quad (3b)$$

The receiver then combines the even- and odd-time signals in (3) for the STLC decoding as follows [7]–[11]:

$$y_{1,2k'-1}[t] + y_{2,2k'}^*[t] = \alpha[t]x_{2k'-1}[t] + v_{1,2k'-1}[t] + v_{2,2k'}^*[t], \quad (4a)$$

$$-y_{1,2k'}[t] + y_{2,2k'-1}^*[t] = \alpha[t]x_{2k'}[t] - v_{1,2k'}[t] + v_{2,2k'-1}^*[t], \quad (4b)$$

where $\alpha[t]$ is the effective channel gain of the t th RB that is defined as $\alpha[t] = \sum_{n=1}^N \|\mathbf{h}_n[t]\|$.

As shown in [7]–[11], with the knowledge of the partial CSI, i.e., $\alpha[t]$, instead of the full CSI, a simple maximum-likelihood detector can be applied to independently detect $x_{2k'-1}[t]$ and $x_{2k'}[t]$ from the combined signals (4a) and (4b), respectively. The effective channel gain can be blindly estimated [16]. For phase-shift keying (PSK) symbol detection, even $\alpha[t]$ is not required as it does not affect the phase information. In the next section, we propose a machine-learning-based blind-detection method that implicitly learns the effective channel gain $\alpha[t]$ and modulation size M .

III. CLUSTERING-BASED BLIND DECODING METHOD

In this section, we propose a clustering-based decoding method for the blind decoding of the combined STLC signals in (4). For ease of description of the proposed method, in Fig. 1, the examples of the constellation diagrams and clustering results for the 16-quadrature amplitude modulation (QAM) and 8-PSK cases are depicted under various environments and system configurations. From the top to bottom rows, environments are as follows: i) $1/\sigma_v^2 = 30$ dB and $N = 1$ for 16-QAM, ii) $1/\sigma_v^2 = 10$ dB and $N = 1$ for 16-QAM, iii) $1/\sigma_v^2 = 10$ dB and $N = 8$ for 16-QAM, iv) $1/\sigma_v^2 = 30$ dB and $N = 1$ for 8-PSK, and v) $1/\sigma_v^2 = 10$ dB and $N = 1$ for 8-PSK. From the left to right columns, i) $y_{r,k}[t]$, ii) $d_k[t]$, iii) $\bar{d}_k[t]$ with C_m , iv) the clusters with the random-initial cluster centroids and iv) the clusters with the designed initial cluster centroids are shown, whose details will be introduced shortly.

The received STLC signals in (3) appear randomly in the constellation diagram as shown in the first column of Fig. 1. However, combining the STLC signals in (4) removes the phase distortion caused by the channels as shown in the second column in Fig. 1. Let denote the combined STLC signals in (4) by the data samples, $d_k[t]$, as follows ($k = \{1, \dots, K\}$ and $t = \{1, \dots, T\}$): $d_k[t] \triangleq \alpha[t]x_k[t] + v_k[t]$, where if $k = 2k' - 1$, $d_k[t] = y_{1,2k'-1}[t] + y_{2,2k'}^*[t]$ and $v_k[t] = v_{1,2k'-1}[t] + v_{2,2k'}^*[t]$, and if $k = 2k'$, $d_k[t] = -y_{1,2k'}[t] + y_{2,2k'-1}^*[t]$ and $v_k[t] = -v_{1,2k'}[t] + v_{2,2k'-1}^*[t]$. Since the effective channel gain of STLC, i.e., $\alpha[t]$, is a real value, the shape of the constellation points is sustained and phase distortion from the complex-value channels is removed.

The combined STLC signals $\{d_k[t]\}$ are then clustered. As earlier mentioned, the number of clusters is ideally equivalent to the modulation size M , and each cluster index of the signal is uniquely mapped to $\log_2 M$ -bit sequence, which is a decoding (or demodulation) procedure. Here, two questions arisen during the learning system implementation are how to reliably cluster $d_k[t]$ and how to determine the cluster indices to map them uniquely to the binary information sequences. We propose k -mean method¹ with the following five steps and provide the feasible answers.

STEP 1: The first step is a signal normalization step. Because the number of data samples from one RB may not be sufficient to be accurately clustered. For example, if one RB t consists of 168 16-QAM symbols, i.e., $K = 168$, there would be around 16 samples in one cluster, which is insufficient to be clearly clustered if an additive noise is severe. To overcome this issue, the whole data samples of T RBs in a frame are used for the clustering. However, the effective channel gain $\alpha[t]$ for RB t , i.e., $\mathbf{d}[t] = [d_1[t]d_2[t] \cdots d_K[t]]^T$, varies for different RBs (see the second column of Fig. 1, specifically Fig. 1.(a2), in which $\mathbf{d}[1]$ and $\mathbf{d}[2]$ are highlighted by red-color ‘□’ and green-color ‘△’, respectively). Thus, $\mathbf{d}[t]$ needs to be normalized to align all $d_k[t]$'s for all t by suppressing the real-value channel gain $\alpha[t]$ as follows: $\bar{\mathbf{d}}[t] = \mathbf{d}[t] / \|\mathbf{d}[t]\|_F$ for given t , such that $\|\bar{\mathbf{d}}[t]\|_F^2 = 1$ for all t , where $\bar{\mathbf{d}}[t] = [\bar{d}_1[t]\bar{d}_2[t] \cdots \bar{d}_K[t]]^T$ and $\|\cdot\|_F$ is a Frobenius norm of a vector. Throughout the signal normalization step, the channel effect is smoothed out and all data samples, $\bar{d}_k[t]$, $\forall k$ and $\forall t$, can be approximately aligned as shown in the third column of Fig. 1, and they are now ready to be used for the clustering.

The normalization step requires $\mathcal{O}(KT)$ time complexity. Note that the time complexity of the normalization step is independent of the modulation size M .

STEP 2: This step is to determine the number of clusters. There are various clustering validation methods to find the optimal number of clusters according to various metrics, such as the Calinski-Harabasz indices, gap statistics, DB indices and silhouette scores [14], [15]. In this study, the DB index and silhouette score are used as they are proper to the k -mean algorithm [15]. Here, the minimum and maximum sizes of clusters, i.e., the minimum and maximum modulation sizes, are assumed to be known at the receiver, yet the assumption is not necessarily required. The random-initial centroids are used for the initial clustering, where the number of centroids is between the minimum and maximum sizes of possible modulation, denoted by M_{\min} and M_{\max} respectively. If the clustering is perfectly performed without error, the number of clusters through the clustering validation, denoted by \tilde{M} , is identical to the modulation size, i.e., $M = \tilde{M}$.

The time complexity of this step is $\mathcal{O}(KT(M_{\max} - M_{\min} + 1)q)$, where q is the number of iterations for a given cluster size [17]. Note that the number of iterations is smaller than five in our simulation, which is relatively negligible compared to KT , we then omit it from the time complexity and approximate it as $\mathcal{O}(KT(M_{\max} - M_{\min} + 1)q) \approx \mathcal{O}(KTM_{\max})$.

STEP 3: To improve the clustering performance and to label the indices of the clusters in the next step, in the third step, we design \tilde{M} -initial centroids by exploiting the structure of the constellation of the estimated modulation type in Step 2. The random-initial centroids, which are typically used for a traditional k -mean algorithm, cause poor clustering results as shown in the fourth column of Fig. 1), especially when the iteration number is insufficient. Furthermore, after the clustering with the random-initial centroids, it is intractable to label the

¹As shown later, the clusters are supposed to be hypersphere in a constellation diagram, thus, a simple and efficient k -mean algorithm is considered in this study for the clustering.

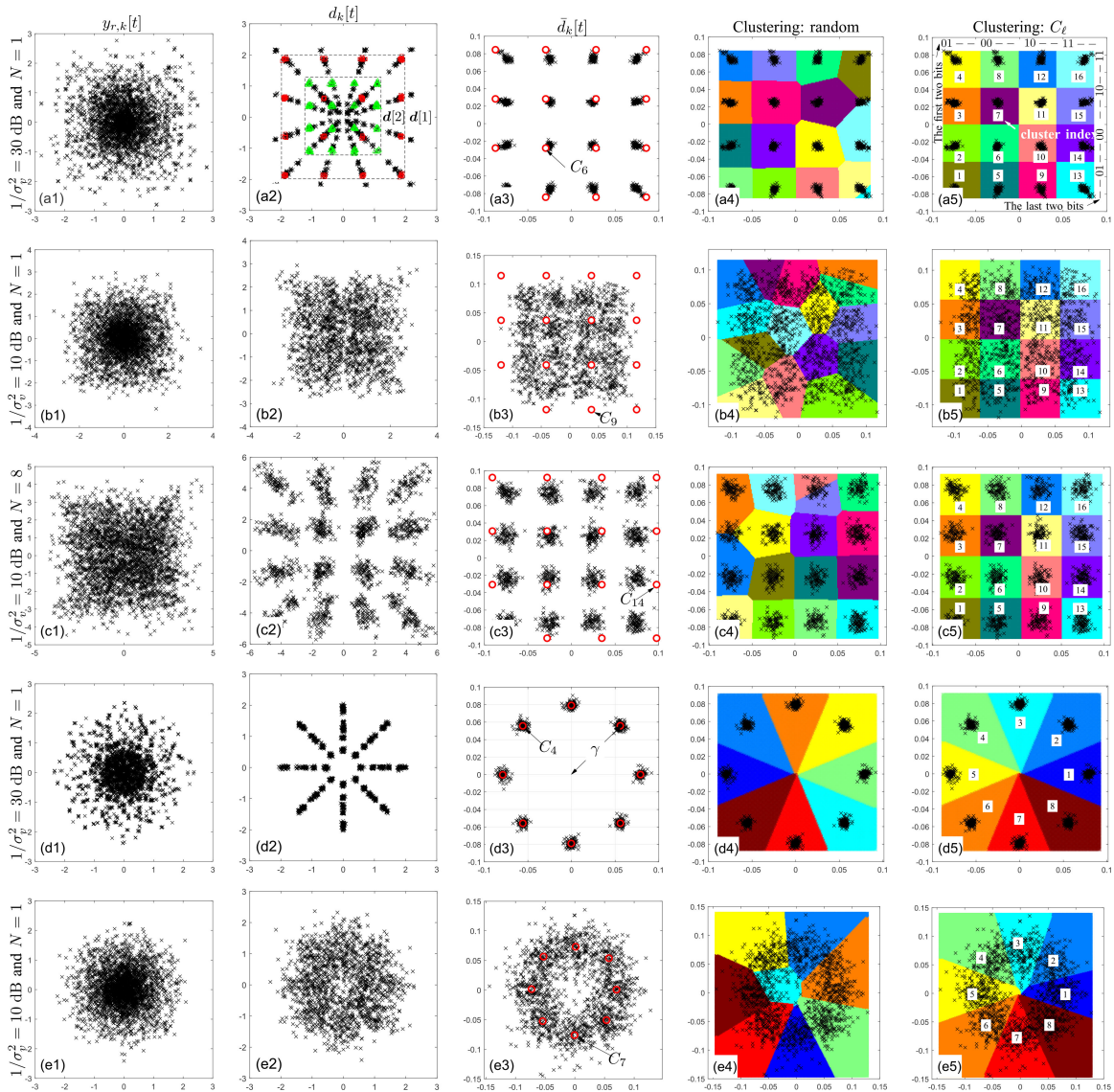


Fig. 1. Constellation diagrams when 16-QAM and 8-PSK modulations are used. From left to right columns, i) $y_{r,k}[t]$, ii) $d_k[t]$, iii) $\bar{d}_k[t]$, and iv) the clusters and corresponding bit sequences are shown. From top to bottom rows, environments are as follows: i) $1/\sigma_v^2 = 30$ dB and $N = 1$ for 16-QAM, ii) $1/\sigma_v^2 = 10$ dB and $N = 1$ for 16-QAM, iii) $1/\sigma_v^2 = 10$ dB and $N = 8$ for 16-QAM, iv) $1/\sigma_v^2 = 30$ dB and $N = 1$ for 8-PSK, and v) $1/\sigma_v^2 = 10$ dB and $N = 1$ for 8-PSK. The x - and y -axes represent the in-phase and quadrature components, respectively.

cluster indices due to the randomness. Since the shape of a constellation of $\bar{d}_k[t]$'s is ideally (i.e., if there is no noise) equivalent to that of the original modulated symbols, we design the initial centroids, denoted by C_ℓ where $\ell = 1, \dots, \tilde{M}$, such that they are scaled version of the original constellation points of the modulated signals.

For example, if $\log_2 \tilde{M}$ is an even number in Step 2, the receiver declares the transmitted signals are the QAM signals, and the initial centroids (a_{m_1}, b_{m_2}) for the QAM signals are designed as follows ($m_1, m_2 \in \{1, \dots, \tilde{M}^{0.5}\}$):

$$a_{m_1} = \min\{\Re(\bar{\mathbf{d}})\} + (m_1 - 1) \frac{\max\{\Re(\bar{\mathbf{d}})\} - \min\{\Re(\bar{\mathbf{d}})\}}{\tilde{M}^{0.5} - 1}, \quad (5a)$$

$$b_{m_2} = \min\{\Im(\bar{\mathbf{d}})\} + (m_2 - 1) \frac{\max\{\Im(\bar{\mathbf{d}})\} - \min\{\Im(\bar{\mathbf{d}})\}}{\tilde{M}^{0.5} - 1}, \quad (5b)$$

where $\bar{\mathbf{d}} = [\bar{d}[1]^T \dots \bar{d}[T]^T]^T$ and $\Re(\bar{\mathbf{d}})$ and $\Im(\bar{\mathbf{d}})$ take the real and imaginary values of $\bar{\mathbf{d}}$, respectively. In Fig. 1(a3), (b3), and (c3), the 'o' mark shows the designed initial centroids from (5) when $\log_2 \tilde{M} = 4$, i.e., 16-QAM signals. The designed initial centroids will be used for the k -mean clustering in the next step and the ℓ th centroid C_ℓ produces cluster ℓ . In other words, the cluster indices, which are shown in Fig. 1(a5), (b5), and (c5), are the same as the centroid indices $\{\ell\}$, which are determined as follows ($m_1, m_2 \in \{1, \dots, \tilde{M}^{0.5}\}$):

$$\ell = \sqrt{\tilde{M}}(m_1 - 1) + m_2. \quad (6)$$

If $\log_2 \tilde{M}$ is an odd number in Step 2, the receiver declares the transmitted signals are the PSK signals, and (a_m, b_m) for the PSK signals are designed as follows ($m = 1, \dots, \tilde{M}$):

$$a_m = \gamma \cos(\theta_m) \text{ and } b_m = \gamma \sin(\theta_m), \quad (7)$$

where $\theta_m = 2\pi(m-1)/\tilde{M}$ and γ is the average distance between the normalized PSK symbols $\{\tilde{d}_k[t]\}$ and the origin in the constellation diagram as shown in Fig. 1(d3). The average distance γ is obtained as $\gamma = \frac{1}{KT} \sum_{t=1}^T \sum_{k=1}^K |\tilde{d}_k[t]|$. The resultant cluster index ℓ from the initial centroid C_ℓ is determined as shown in Fig. 1(d5) and (e5), i.e.,

$$\ell = m, m \in \{1, \dots, \tilde{M}\}. \quad (8)$$

The time complexity of this step is $\mathcal{O}(\tilde{M})$, which is negligible compared to the complexity of Step 2.

STEP 4: With the designed C_ℓ , the k -mean clustering is performed. Here, *squared Euclidian* distance is used as the distance metric. In the fifth column of Fig. 1, all $\tilde{d}_k[t]$'s in a frame are clustered by one iteration of a k -mean algorithm with the designed \tilde{M} -initial centroids, C_ℓ 's. From this example, it is clear that the designed initial centroids provide better clustering performance than the random-initial centroids, whose clustering results with five iterations are shown in the fourth column of Fig. 1. The time complexity of the k -mean clustering for a given number of clusters, i.e., \tilde{M} , is $\mathcal{O}(KT\tilde{M})$ [17].

STEP 5: The last step is to map the cluster indices of the data samples to the corresponding binary sequences, i.e., information bits. This step can be interpreted as a decoding or demodulation step. For example, in Fig. 1(a5), if $\tilde{d}_k[t]$ is a member of cluster '7', the decoded bits for the k th transmitted symbol in the t th RB will be '0010.' In other words, the receiver decodes the equivalent combined STLC signal $x_k[t]$ in (4) to '0010.'

The time complexity of the mapping step is $\mathcal{O}(1)$.

Remark 1: The overall time complexity from Step 1 to Step 5 is $\mathcal{O}(KT + KT M_{\max} + \tilde{M} + KT\tilde{M} + 1) \approx \mathcal{O}(KT M_{\max})$, which is comparable to the time complexity $\mathcal{O}(KT M)$ of the conventional coherent decoding systems.

Remark 2: The proposed scheme using unsupervised learning, i.e., a clustering, is independent of the SNR. However, the supervised learning methods, such as k -nearest neighbors (k -NN) and an SVM, require to train for each modulation type under a given SNR condition. To learn all possible modulation types and to cover the whole SNR regime, the training period could be prohibitively large, which hinders the receiver from employing the supervised learning methods.

IV. SIMULATION RESULTS AND DISCUSSION

In this section, the BER performance of the proposed k -mean-based blind decoding scheme is evaluated. The squared Euclidian distance is used for cluster validation and clustering. If a cluster loses all its member observations, a new cluster that consists of the one point furthest from its centroid is generated during the clustering. Clustering starts with the initial cluster centroids designed in Step 3, and does not use any new initial cluster centroids until the clustering is completed. Each observation is assigned to the cluster with the closest centroid, i.e., a batch update for low time complexity. The maximum number of iterations is set to be 10. One RB consists of 168 16-QAM symbols and the number of RBs per frame is set as $T = 10$ RBs by referring to 5G new radio frame structure [19]. The number of transmit antennas is set as $N \in \{1, 2, 4, 8\}$. The list of the number of clusters in the cluster validation includes all possible modulation types, i.e., \tilde{M} , and it is designed and shared between transmitter and receiver as in an adaptive modulation system [18]. In our simulation, we set the list by $\{1, 2, 3, 4, 16, 64\}$. Here, $\tilde{M} = 1$ and $\tilde{M} = 3$ is for BPSK and 8-PSK, respectively, and the others are for QAM. If there is no common information regarding the possible modulation types, the list includes

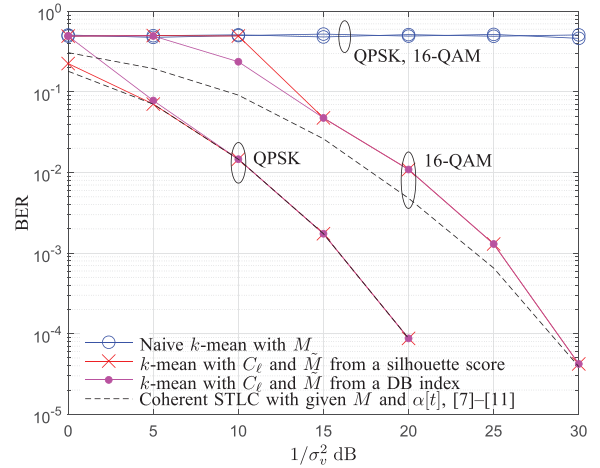


Fig. 2. BER performance (QPSK and 16-QAM) over $1/\sigma_v^2$ when $N = 1$.

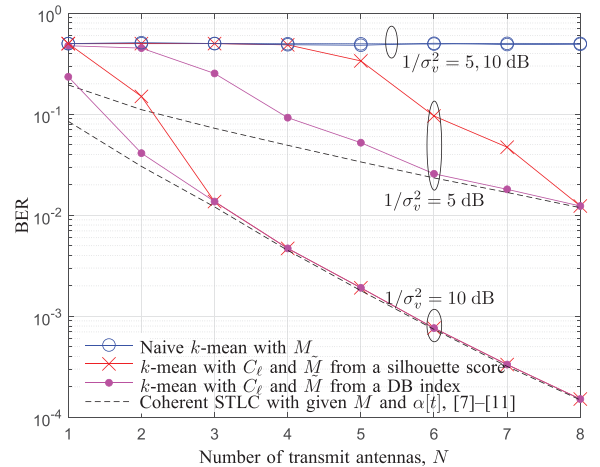


Fig. 3. BER performance (16-QAM) over N when $1/\sigma_v^2 = \{5, 10\}$ dB.

the integers starting from one to M_{\max} as large as possible depending on the system computational capability. The following methods are compared:

- Naive k -mean that starts with a random centroid and with given M (similar results without given M are omitted).
- k -mean with initialized centroids, C_ℓ , and \tilde{M} obtained from a silhouette score, where the overall silhouette value is computed for the clustering solution by averaging the silhouette values for all points, and each cluster contributes to the overall silhouette value proportionally to its size.
- k -mean with initialized centroids, C_ℓ , and \tilde{M} obtained from a DB index.
- Coherent STLC as a benchmarking method, i.e., an STLC system with given M and $\alpha[t]$ [7]–[11].

In Fig. 2, the BER is evaluated across $1/\sigma_v^2$ when the transmitter has one antenna, i.e., $N = 1$. From the results, we see that the initial cluster centroids are critical to properly cluster the data symbols. Note that the naive k -mean algorithm with the random-initial centroids provides very poor performance because of the random indexing and corresponding incorrect mapping, regardless of the knowledge of the exact modulation size M . However, using the designed initial cluster centroids, C_ℓ , the k -mean provides the similar BER trend to the coherent decoding

that knows exact M and $\alpha[t]$. When $M = 4$, a DB index provides the accurate M than a silhouette score, while when $M = 2$, the silhouette score outperforms the DB index. When the modulation size is small, i.e., $M = 2$, both clustering evaluation methods perfectly estimate the number of clusters, as a result, coherent decoding performance is obtained when $1/\sigma_v^2 \geq 5$ dB. However, for 16-QAM, $1/\sigma_v^2$ greater than 30 dB is required for the coherent decoding performance. This requirement can be relaxed by using more transmit antennas, which increases $\alpha[t]$ and improve clustering performance. This is verified in Figs. 1 and 3.

In Fig. 3, the BERs are shown by varying the number of transmit antennas, when 16-QAM symbols are transmitted and $1/\sigma_v^2 = \{5, 10\}$ dB. From this results, it is verified that the proposed k -mean-based blind decoding method can achieve near coherent decoding performance if the transmitter has multiple antennas more than two for $1/\sigma_v^2 = 10$ dB and five for $1/\sigma_v^2 = 5$ dB.

V. CONCLUSION

In this paper, a novel k -mean-based decoding method with the initial cluster centroids was proposed for the blind decoding of the STLC symbols. From the numerical results, it was verified that the proposed blind decoding method can achieve almost coherent decoding performance, especially, when the modulation size is small and/or the number of transmit antennas is sufficiently large. The proposed blind decoding method is expected to be applied to the various STLC schemes.

REFERENCES

- [1] J. Joung, "Machine learning-based antenna selection in wireless communications," *IEEE Commun. Lett.*, vol. 20, no. 11, pp. 2241–2244, Nov. 2016.
- [2] Y. Liu, S. Cheng, and Y. Hsueh, "eNB selection for machine type communications using reinforcement learning based Markov decision process," *IEEE Trans. Veh. Technol.*, vol. 66, no. 12, pp. 11330–11338, Dec. 2017.
- [3] B. Mao *et al.*, "A novel non-supervised deep-learning-based network traffic control method for software defined wireless networks," *IEEE Wireless Commun.*, vol. 25, no. 4, pp. 74–81, Aug. 2018.
- [4] G. Gui, H. Huang, Y. Song, and H. Sari, "Deep learning for an effective nonorthogonal multiple access scheme," *IEEE Trans. Veh. Tech.*, vol. 67, no. 9, pp. 8440–8450, Sep. 2018.
- [5] F. Tang, B. Mao, Z. M. Fadlullah, and N. Kato, "On a novel deep-learning-based intelligent partially overlapping channel assignment in SDN-IoT," *IEEE Commun. Mag.*, vol. 56, no. 9, pp. 80–86, Sep. 2018.
- [6] H. Huang, J. Yang, Y. Song, H. Huang, and G. Gui, "Deep learning for super-resolution channel estimation and DOA estimation based massive MIMO system," *IEEE Trans. Veh. Technol.*, vol. 67, no. 9, pp. 8549–8560, Sep. 2018.
- [7] J. Joung, "Space-time line code," *IEEE Access*, vol. 6, pp. 1023–1041, 2018.
- [8] J. Joung, "Space-time line code for massive MIMO and multiuser systems with antenna allocation," *IEEE Access*, vol. 6, pp. 962–979, 2018.
- [9] J. Joung, "Energy efficient space-time line coded regenerative two-way relay under per-antenna power constraints," *IEEE Access*, vol. 6, pp. 47026–47035, 2018.
- [10] J. Joung and E.-R. Jeong, "Multiuser space-time line code with optimal and suboptimal power allocation methods," *IEEE Access*, vol. 6, pp. 51766–51775, 2018.
- [11] J. Joung and J. Choi, "Uneven power amplifier shuffling for space-time line code (STLC) systems," *IEEE Access*, vol. 6, pp. 58491–58500, 2018.
- [12] J. H. Lee, J. Kim, B. Kim, D. Yoon, and J. W. Choi, "Robust automatic modulation classification technique for fading channels via deep neural network," *Entropy*, vol. 19, pp. 1–11, 2017.
- [13] E. Alpaydin, *Introduction to Machine Learning*, 3rd ed. Cambridge, MA, USA: MIT Press, 2014.
- [14] N. Bolshakova and F. Azuaje, "Cluster validation techniques for genome expression data," *Signal Process.*, vol. 83, pp. 825–833, Apr. 2003.
- [15] S. Petrović, "A comparison between the Silhouette index and the Davies-Bouldin index in labelling IDS clusters," in *Proc. 11th Nordic Workshop Secure IT-Syst.*, Sweden, Oct. 2006, pp. 1–12.
- [16] P. Gao and C. Tepedelenlioglu, "SNR estimation for nonconstant modulus constellations," *IEEE Trans. Signal Process.*, vol. 53, no. 3, pp. 865–870, Mar. 2005.
- [17] M. K. Pakhira, "A linear time-complexity k -means algorithm using cluster shifting," in *Proc. Int. Conf. Comput. Intell. Commun. Netw.*, Bhopal, 2014, pp. 1047–1051.
- [18] S. Catreux, V. Erceg, D. Gesbert, and R. W. Heath, "Adaptive modulation and MIMO coding for broadband wireless data networks," *IEEE Commun. Mag.*, vol. 40, no. 6, pp. 108–115, Jun. 2002.
- [19] X. Lin *et al.*, "5G new radio: Unveiling the essentials of the next generation wireless access technology," Jun. 2018, arXiv:1806.06898v1.